Journal of Fluorine Chemistry 132 (2011) 703–712

Contents lists available at ScienceDirect

Journal of Fluorine Chemistry

journal homepage: www.elsevier.com/locate/fluor

Aluminium(III) fluoride originating from decomposition of hydrazinium fluoroaluminate(III) under oxidative conditions: Syntheses, X-ray photoelectron spectroscopy and some catalytic reactions

Tomaž Skapin [a,*], Zoran Mazej [a], Anna Makarowicz [b], Adolf Jesih [a], Mahmood Nickkho-Amiry [c], Sven L.M. Schroeder [b,d], Norbert Weiher [b], Boris Žemva [a], John M. Winfield [c]

[a] Department of Inorganic Chemistry and Technology, Jožef Stefan Institute, Jamova 39, SI-1000 Ljubljana, Slovenia
[b] School of Chemical Engineering and Analytical Science, The University of Manchester, The Mill, Manchester M13 9PL, UK
[c] Department of Chemistry, University of Glasgow, Joseph Black Building, Glasgow G12 8QQ, UK
[d] School of Chemistry, The University of Manchester, Oxford Road, Manchester M13 9PL, UK

ARTICLE INFO

Article history:
Received 26 January 2011
Received in revised form 22 April 2011
Accepted 22 April 2011
Available online 30 April 2011

Dedicated to Dr. Alain Tressaud, recipient of the 2011 ACS Award for Creative Work in Fluorine Chemistry.

Keywords:
Aluminium fluoride
Oxidative decomposition
XPS
Catalysis
[^{36}Cl]-radiotracer

ABSTRACT

Decomposition of hydrazinium pentafluoroaluminate under oxidative (F_2) conditions leads to aluminium(III) fluoride whose properties are highly dependent on the conditions used for synthesis. In the presence of anhydrous HF, which probably acts as a heat exchange agent, samples have high BET areas, whereas BET areas of samples prepared under gas–solid conditions are small. XPS data are consistent with the presence of Lewis acid centres but, more importantly, emphasise the importance of surface hydroxyl groups, particularly in high surface area compounds. Catalytic behaviour towards isomerisation of 1,1,2-trichlorotrifluoroethane and subsequent dismutations at moderate temperatures and towards room temperature dehydrochlorination of *tert*-butyl chloride has been demonstrated for some high BET samples; both reactions indicate that surface Lewis sites exist. Catalytic ability is inhibited by surface hydroxyl groups but is improved by prior fluorination of the surface with CCl_2F_2. Catalysis is inhibited also by the presence of ammonium fluoroaluminate, a by-product of the decomposition process. The $[NH_4]^+$ salt level can be reduced by washing with anhydrous HF.

1. Introduction

Solid, binary metal fluorides that are prepared *via* conventional means characteristically have small specific surface areas, since, in most cases, their lattices are close packed arrays of fluoride with metal atoms occupying various arrangements of octahedral or tetrahedral holes. However, the recent development of non-aqueous sol–gel routes as a way of preparing metal fluorides having very small particle size has led to the formation of amorphous materials, which have rather large specific surface areas, for example BET areas in the 10^2 m^2 g^{-1} range. There has been particular interest in aluminium [1] and magnesium [2] fluorides (HS-AlF_3 and HS-MgF_2) prepared by this route and many of their properties have been investigated. In particular, these materials have significant Lewis acidities from which Brønsted acidity can be induced by surface hydroxylation, due either to adventitious water or deliberate water contact during synthesis. The versatile catalytic applications of HS-AlF_3, HS-MgF_2 and their hydroxylated derivatives have been recently reviewed [3].

Development of the chemistry of corresponding aluminium fluorides, using a purely inorganic preparation route as an alternative to the sol–gel process, is the subject of the present report. Some of the properties of these solids, in particular their XPS spectra and their behaviour as heterogeneous catalysts, are compared with the analogous behaviour of sol–gel synthesised HS-AlF_3.

Hydrazinium compounds are used as starting substances since thermal decomposition of hydrazinium fluorometallates offers a convenient route for the preparation of binary fluorides. For example, the hydrazinium fluoroaluminates(III), $[N_2H_5]_3[AlF_6]$ [4] and $[N_2H_6][AlF_5]H_2O$ [5], decompose to give pure α-AlF_3 as the final product at elevated temperatures. Despite numerous reports of thermal decomposition studies involving hydrazinium fluorometallates, no systematic studies of particle dimensions or specific surface area of the final products appear to have been undertaken. Thermal decomposition of hydrazinium salts usually proceeds to give binary fluorides and ammonium fluorometallates

* Corresponding author. Tel.: +386 1 477 3557; fax: +386 1 477 3155.
E-mail address: tomaz.skapin@ijs.si (T. Skapin).

0022-1139/$ – see front matter © 2011 Elsevier B.V. All rights reserved.
doi:10.1016/j.jfluchem.2011.04.013

as intermediate products. Ammonium fluorometallates decompose to give pure binary fluorides only at relatively high temperatures. Even at *ca.* 1100 K some residual $[NH_4]^+$ can be present. Such a high temperature is not favourable for the preparation of materials with high surface areas and, for this reason, the possibility of decomposing hydrazinium pentafluoroaluminate(III) by strong oxidizers at room temperature has been explored. A short account of this route has recently appeared and the nanoscopic nature of some of the products demonstrated by electron microscopy, particularly TEM [6].

The Lewis acid properties of the AlF_3 materials prepared in the present work have been examined by pyridine adsorption monitored by FTIR spectroscopy [6] and now through X-ray photoelectron spectroscopic (XPS) analysis in order to permit comparisons with analogous data from sol–gel prepared HS-AlF_3 [7,8]. Finally, the behaviour of the materials as possible catalysts in two reactions, isomerisation of 1,1,2-trichlorotrifluoroethane and the room temperature dehydrochlorination of *tert*-butyl chloride is examined. These reactions are among several that have been used as operational tests for Lewis acidity in HS-AlF_3 and related binary fluorides [3,9].

2. Experimental

2.1. Synthesis of $[N_2H_6][AlF_5]$

Hydrazinium pentafluoroaluminate, $[N_2H_6][AlF_5]$, was prepared by mixing aqueous solutions of $N_2H_6F_2$, prepared from $N_2H_4{\cdot}H_2O$ and HF, and $AlF_3{\cdot}3H_2O$ in a polyethylene beaker according to the known procedure [10]; the product precipitated as a white polycrystalline material. It was filtered, dried under dynamic vacuum at room temperature and stored in a glove box. Before some decomposition runs, $[N_2H_6][AlF_5]$ samples were dried additionally at 333, 363, 388 or 393 K. Chemical analyses, X-ray powder diffraction, FTIR and Raman spectroscopy indicated that the product was $[N_2H_6][AlF_5]$ containing up to 2 wt.% of water. Several 10 g batches were prepared with good repeatability. Analyses, Found Al, 16.7–17.0; F, 58.7–59.7; N_2H_6, 21.8–22.5%. $[N_2H_6][AlF_5]$ req. Al, 17.3; F, 60.9; N_2H_6, 21.8%.

2.2. Preparation procedures

2.2.1. Fluorination of γ-alumina

Fluorinated γ-Al_2O_3 has been used as a benchmark to compare catalytic activity in conventionally prepared, aluminium fluoride derivatives [11–13]. It had a similar function in the present work and was prepared from commercial γ-alumina pellets (Shell S 618) having nominal diameter 0.8 mm and a specific surface area of 240 $m^2\ g^{-1}$. Pellets were preconditioned in flow of nitrogen at 623 K for 3 h and then fluorinated by a flow of trifluoromethane, CHF_3, at 623 K for 3 h. Other reference materials, aluminium chlorofluoride (ACF), $AlCl_xF_{3-x}$, $x = 0.13$) [14,15], HS-AlF_3, prepared by sol–gel synthesis [1], and the hexagonal tungsten bronze, β-AlF_3 [16], were provided by E. Kemnitz, HU-Berlin and were used as received.

CAUTION! The following preparation procedures include the use of anhydrous hydrogen fluoride (aHF) and fluorine (F_2). Both chemicals are highly toxic and potentially dangerous. They must be handled with high precaution by using appropriate apparatus and protective clothing.

2.2.2. Oxidative decomposition reactions of $[N_2H_6][AlF_5]$ under gas–solid conditions

These were performed batchwise in tubular copper or stainless steel reactors of 50 mm i.d. and 100–600 ml volume. Fluorine (Solvay, 98%) was used as received. It was dosed in portions as 5, 10 or 30% mixtures with argon, dinitrogen or as pure F_2 gas. Solid $[N_2H_6][AlF_5]$ in 0.37, 0.5 or 1.0 g portions was bulk packed or spread over 40, 80 or 120 cm^2 plates. Aluminium(III) fluoride products obtained under gas–solid conditions are denoted as GS-materials.

2.2.3. Oxidative decomposition reactions of $[N_2H_6][AlF_5]$ in the presence of liquid aHF

These were carried out by loading $[N_2H_6][AlF_5]$ aliquots (1.0–17.0 g) in a glove box into 40 ml FEP (tetrafluorethylene–perfluorpropylene) or, 250 and 700 ml Kel-F® (polychlorotrifluoroethylene) reaction vessels. The liquid medium, anhydrous hydrogen fluoride, aHF (10–250 cm^3) and a small portion of fluorine were added at 77 K. Anhydrous HF (Fluka, Purum) had been treated with K_2NiF_6 (Ozark-Mahoning) for several hours prior to use. The frozen reaction mixture was placed in an ultrasonic bath and brought to room temperature. Some experiments were performed without the use of ultrasound. In later experiments reaction mixtures were mixed by means of a magnetic stirrer or a mechanical shaker. After 1 h new portions of fluorine were added until the final pressure in the reaction vessel reached 0.5 MPa. After one day the reaction vessel was cooled to 77 K and volatiles were pumped away. Fluorine was added again till the pressure inside the reaction vessel reached 0.5 MPa. This procedure was repeated several times. The total amount of F_2 added was in *ca.* 10% stoichiometric excess according to Eq. (1).

$$[N_2H_6][AlF_5] + 2F_2 \rightarrow AlF_3 + N_2 + 6HF \quad (1)$$

The mixture was allowed to stand for *ca.* 24 h after the last F_2 addition, then HF and other volatiles were pumped off at ambient temperature. In some experiments the liquid phase (aHF) was decanted prior to evacuation at ambient temperature.

Before characterisation, all solid products were pumped in vacuo at 523 K for several hours to remove HF and other volatile products. Related mass losses during this stage were in the range 5–10%. The AlF_3 products obtained from this procedure in a liquid aHF medium are denoted as LHF-materials.

2.3. Characterisation

As the quantities of products from some batches of oxidative decomposition, from both procedures but especially from gas–solid reactions, were often less than 1 g, complete characterisation of each small batch was not possible. For this reason, a large number of preparations was carried out to ensure the reproducibility of a particular physical or spectroscopic property measured.

2.3.1. Elemental analysis

Aluminium was determined by back titration with 1,2-*cyclo*hexylenedinitrilotetraacetic acid (CDTA) after removal of fluorine from the sample [17]. Total fluorine was determined using a fluoride ion selective electrode [18,19], after complete decomposition of the sample by alkali fusion using $KNaCO_3$. Water content was determined by Karl Fischer titration [20] and ammonia spectrophotometrically after distillation from alkaline media [20,21].

2.3.2. Surface area determination

Specific surface areas were determined by a single-point BET method using a Micromeritics FlowSorb II 2300 instrument and N_2 adsorption at 77 K. Prior to analysis, samples were additionally evacuated at 523 K for several hours and conditioned under N_2 flow at the same temperature for 1 h in the test tube of the FlowSorb instrument.

2.3.3. Powder X-ray diffraction (XRD)

X-ray powder diffraction photographs were obtained using the Debye–Scherrer technique with Ni-filtered Cu K_α radiation. Samples were loaded into quartz capillaries (0.3 mm) in a dry-box. Intensities were estimated visually. X-ray powder diffraction photos of AlF_3, prepared by oxidative decomposition of $[N_2H_6][AlF_5]$ in the presence of liquid aHF showed only two weak, broad lines from which it was not possible to identify the AlF_3 phase(s) formed.

2.3.4. Infrared spectroscopy

Infrared spectra were recorded on a Perkin–Elmer Spectrum GX FTIR spectrometer equipped with MTEC Model 300 photoacoustic detector. During the transfer to the photoacoustic cell, samples were for a short time in contact with ambient air. All spectra were normalised against the strong bands due to Al–F stretching vibrations *ca.* 660 cm^{-1}.

2.4. X-ray photoelectron spectroscopy

XPS data were acquired with a KRATOS Axis Ultra system. The equipment was fitted with a monochromatic Al K_α X-ray source and a spherical mirror electron analyser. High-resolution scans of Al 2p, F 1s, O 1s and C 1s were taken on an energy grid of 0.1 eV and with a pass energy of 20 eV. Data acquisition times per spectrum were approximately 10 min. Most of the XPS measurements were repeated once or twice with the same set of samples in order to be able to assess reproducibility and the effects of beam damage. The analysis of the data was carried out by unconstrained fitting of two Gaussian/Lorentzian (with a 20% Lorentzian component) peaks in the CasaXPS package [22]. The C 1s emission from adventitious carbon at 284.8 eV was used as the binding energy reference [23]. For several of the spectra (most of the O 1s data, Al 2p of LHF-15, F 1s of LHF-12) the spectra could be equally well fitted with a single peak, and these are the fits that will be presented. For several of the F 1s spectra (LHF-14, LHF-15, GS-13) the two-peak fitting procedure optimised with both peaks at very close binding energies, but with strongly differing FWHM values. As will be explained below, this is a strong indication that the morphology of the samples is heterogeneous, probably with a crystalline minor fluoride phase (low FWHM) alongside a disordered (high FWHM) dominant phase.

2.5. Catalytic activity tests

2.5.1. Isomerisation of 1,1,2-trichlorotrifluoroethane and subsequent dismutation reactions

The behaviour of AlF_3- and reference-materials as heterogeneous catalysts in CCl_2FCClF_2 isomerisation and subsequent reactions was examined under steady flow conditions with a catalytic rig similar to that used in previous investigations using fluorinated aluminas or β-AlF_3 as catalysts [13,24]. The feed, CCl_2FCClF_2, was contained in a thermostated saturator; its concentration and flow were set to the selected values by adjusting the flows of the diluent and feed N_2 and the temperature of the CCl_2FCClF_2 saturator. Flows of N_2 were regulated by mass flow controllers. Diluted CCl_2FCClF_2 entered a nickel tubular catalytic reactor with a fixed bed of catalyst. Exhaust lines were heated to prevent the condensation of less volatile products. Products were analysed using a Perkin–Elmer gas chromatograph with FID detector. Separation of the products was achieved using a packed column (Fomblin YR on Carbopack B) that separated the volatile fractions, $CClF_2CF_3$, CCl_2FCF_3, CCl_2FCClF_2 and CCl_2FCCl_2F, including the corresponding isomers. The product AlF_3 materials were used, when possible, as-prepared in the form of fine powders. In some cases, however, granulation was necessary to prevent excessive pressure drops over the catalyst bed. The quantity of catalysts used was usually in the range of 100–150 mg with the catalyst beds 1–1.5 cm in length. Before tests, catalysts were conditioned *in situ* at 572 K under N_2 flow for 1 h. The concentration of CCl_2FCClF_2 in the feed stream was 10 vol.% and flows were adjusted to obtain a 1 s residence time. Catalytic tests were carried out in two consecutive stages: in the first stage temperature was steeply increased in the range 473–623 K (activation), in the second stage temperature was reduced to 573 K, some of the most active catalysts were also tested at lower temperatures, down to 423 K. GC analyses of the products were obtained after 40 min at the specified temperature to allow equilibration.

2.5.2. Room temperature dehydrochlorination of tert-butyl chloride and [^{36}Cl]-labelled tert-butyl chloride

The principles which underlie the use of [^{36}Cl]-labelled anhydrous hydrogen chloride and *tert*-butyl [^{36}Cl]-chloride to investigate adsorption phenomena and reactions at Lewis acid surfaces such as ACF have been described elsewhere [25]. The procedures used for preparation of [^{36}Cl]-labelled materials and for Geiger–Müller direct monitoring of a surface at which labelled material had been deposited were identical to those recently described for experiments [9,26] that involved HS-AlF_3 and HS-MgF_2, in both cases synthesised *via* the sol–gel route, and aluminium hydroxy fluorides having the hexagonal tungsten bronze structure.

Samples of AlF_3 (220–450 mg) were transferred from Ljubljana to Glasgow in individually heat-sealed FEP ampoules. A sample was transferred to a previously flamed out Pyrex ampoule fitted with a P.T.F.E./Pyrex vacuum stop cock (J. Young) and standard joint by means of which the ampoule was fitted to the Pyrex G.M. counting vessel [25] or to a gas IR cell, for monitoring HCl evolution to the gas phase with time when Bu^tCl contacted the solid [9]. Sample handling procedures, vacuum line and glove box, throughout were designed to avoid contact with moist laboratory air.

3. Results and discussion

3.1. Syntheses

Decomposition of hydrazinium pentafluoroaluminate(III) in the presence of the strongly oxidising fluorine can be achieved at or slightly above room temperature. The thermodynamic driving force for the process results from the exothermic combination of the strong oxidant F_2 with the strongly reducing $[N_2H_6]^{2+}$ cation. In the absence of other factors this reaction, Eq. (1), is difficult to control. Two different approaches were attempted: (i) by performing the reaction under heterogeneous gas–solid conditions, in some reactions the solid being spread thinly on a metal plate, or (ii), under homogeneous conditions in anhydrous hydrogen fluoride (aHF). Details of representative reactions carried out under each set of conditions are given in Table 1. The codes GS- and LHF- indicate samples prepared under gas–solid and in aHF respectively, the numbers being allocated sequentially for each series. Irrespective of the precise conditions used, for example F_2:N_2 ratio in the GS-series or product work-up method in the LHF-series, solids whose Al:F atomic ratios were close to 1:3 were usually obtained. Samples with higher F-contents are presumed to be the result of incomplete HF removal; but more significantly, in determining subsequent behaviour, was the detection of the $[NH_4]^+$ cation in some samples (GS-5, LHF-15 in Table 1). FTIR examination confirmed this finding. Species containing $[NH_4]^+$ are the main side products from oxidative decomposition of hydrazinium precursors. In a deficiency of fluorine, incomplete

Table 1
Preparation conditions and properties of the aluminium fluoride samples.

Sample	Synthesis conditions and post-treatment regime	Analysis/wt.% and atomic ratio	BET area/$m^2\,g^{-1}$
F–Al_2O_3 (ref. compd.)	Commercial γ-Al_2O_3 fluorinated with CHF_3 at 623 K; at 623 K in N_2 for 1 h	F, 58.4	34
GS-5	Dry $N_2H_6AlF_5$ with 10% F_2 in Ar at 333 K using 0.37 g bulk-packed; at 523 K in vacuo for 4 h	Al, 30.9; F, 65.1; NH_4, <0.2 Al:F = 1:2.99	41
GS-13	Dry $N_2H_6AlF_5$ with 100% F_2 at 333 K using 0.5 g spread on plates		26
GS-14	Dry $N_2H_6AlF_5$ with 100% F_2 at 423 K using 0.6 g bulk-packed; at 523 K in vacuo for 4 h		44
GS-16	Dry $N_2H_6AlF_5$ with 100% F_2 at 333 K with 1.0 g spread on plates		23
GS-18	100% F_2 at 333 K with 0.5 g spread on plates		25
GS-33	100% F_2 at 333 K with 1.0 g spread on plates		22
LHF-8	$N_2H_6AlF_5$ dried at 363 K, 50 ml reactor, HF pumped off after reaction		280
LHF-12	$N_2H_6AlF_5$ dried at 363 K, 50 ml reactor, after reaction HF decanted and then pumped; at 523 K in vacuo for 4 h	Al, 29.7; F, 66.3 Al:F = 1:3.17	276
LHF-14	$N_2H_6AlF_5$ dried at 363 K, 700 ml reactor, HF pumped off after reaction; at 523 K in vacuo for 4 h	Al, 30.8; F, 63.7 Al:F = 1:2.94	211
LHF-15 (raw product)	$N_2H_6AlF_5$ dried at 363 K, 700 ml reactor, HF pumped off after reaction	Al, 26.4; F, 66.5 Al:F = 1:3.58	
LHF-15	LHF-15 raw product in vacuo at 523 K	Al, 29.5; F, 64.5; NH_4, 1.3 Al:F:NH_4 = 1:3.11:0.07	267
LHF-15a	LHF-15 extracted with HF		
LHF-15b	LHF-15 treated in HF with F_2 under UV, HF decanted		270
LHF-16	$N_2H_6AlF_5$ dried at 393 K, 250 ml reactor cooled to 273 K, HF decanted and then pumped	A, 29.9; F, 65.3 Al:F = 1:3.10	217
LHF-16a	LHF-16 treated with CCl_2F_2 at 623 K	Al, 30.7; F, 64.8 Al:F = 1:2.99	125

decomposition may take place according to Eqs. (2) and (3).

$$2[N_2H_6][AlF_5] + F_2 \rightarrow 2[NH_4][AlF_4] + N_2 + 4HF \quad (2)$$

$$2[N_2H_6][AlF_5] + F_2 \rightarrow 2[NH_4]F + 2AlF_3 + N_2 + 4HF \quad (3)$$

Volatile $[NH_4]F$ is largely removed by evacuation at 523 K, a routine post-treatment performed after each decomposition step. It is therefore very likely that residual $[NH_4]^+$ found in some AlF_3 samples was present as non-volatile $[NH_4][AlF_4]$, formed according to Eq. (2), or from an acid–base reaction between $[NH_4]F$ and highly active, high surface AlF_3. In independent experiments, decomposition of $[NH_4][AlF_4]$ by fluorine was shown to occur to a considerable extent above 473 K with the formation of low surface area α-AlF_3. In the absence of F_2, thermal decomposition of $[NH_4][AlF_4]$ occurs above 723 K with the formation of β-AlF_3 [27]. Formation of α-AlF_3 in the decomposition by fluorine may be associated with the strongly exothermic nature of this reaction. During decomposition, temperatures at the molecular level may considerably exceed the nominal reaction temperature leading to the formation of the thermodynamically most stable phase, α-AlF_3. In contrast, thermal decomposition of $[NH_4][AlF_4]$ is an endothermic process that at temperatures below 803 K favours the formation of the metastable β-AlF_3 phase. Both processes for residual $[NH_4][AlF_4]$ elimination mentioned above, reaction with fluorine and thermal decomposition, are effective under relatively severe conditions that would inevitably alter the structure of the amorphous AlF_3 phase and ultimately result in a considerable reduction of the surface area. Strategies to reduce $[NH_4][AlF_4]$ at milder conditions were therefore investigated and are described in Section 3.3.1.

The most striking difference between GS- and LHF-samples is their BET areas. The former are relatively small, 22–44 $m^2\,g^{-1}$, which are comparable to that of the benchmark fluorinated γ-alumina (Table 1), while the latter are significantly larger, 211–280 $m^2\,g^{-1}$. However, treatment with CCl_2F_2, a precursor to a catalytic test, led to a reduction in BET area (LHF-16 vs. LHF-16a in Table 1). Although in neither group were the materials truly crystalline, there was some evidence for some of the GS-samples that α- or β-AlF_3 phases were present. When reaction conditions are not controlled, the product is largely α-AlF_3. Based solely on powder X-ray diffraction results, LHF-samples with large surface area can be regarded as amorphous. However, TEM demonstrates that some structural order is present since they consist of an amorphous phase and nanocrystalline phases of α- and β-AlF_3 [6].

3.2. XPS analysis

XP spectra of HS-AlF_3 samples prepared by the non-aqueous sol–gel route have previously been reported in some detail [7,8] with the aim of understanding the origins of characteristically high acidity (both Lewis and Brønsted) of these materials. Although simple correlations between BE values or the areas under BE peaks are not possible [8] it is clear that variations in local geometric structures are responsible for the strong Lewis acid sites, as they result in better exposure of potential reagent species to the surface acid sites. It has also been concluded that dangling or bridging hydroxyl groups have a key role in the establishment of Brønsted acidity [8], but there was no evidence for dangling surface F-atoms in experimental data for HS-AlF_3 materials [8]. Similar considerations are expected for the samples examined here.

Spectra and fits of selected high surface area (LHF) and low surface area (GS) samples are given in Fig. 1. The parameters obtained from the fitting analysis are given in Tables 2 and 3 respectively.

3.2.1. High surface area (LHF) samples

The dominant Al 2p emission components of samples treated post-synthesis occur at similar binding energies, 76.7 eV for LHF-14 and 76.3 eV for LHF-12 (Table 2, Fig. 1). These binding energy values are close to the Al 2p binding energy observed for crystalline α-AlF_3 [8,28]. The remaining sample, LHF-15, which was not treated after synthesis, has a single emission feature at a lower Al 2p binding energy, 75.9 eV, indicating incomplete fluorination and a non-stoichiometric surface composition [8,28]. Without evacuation after synthesis, HF is likely to remain strongly adsorbed, together with the ubiquitous hydroxylic surface species and

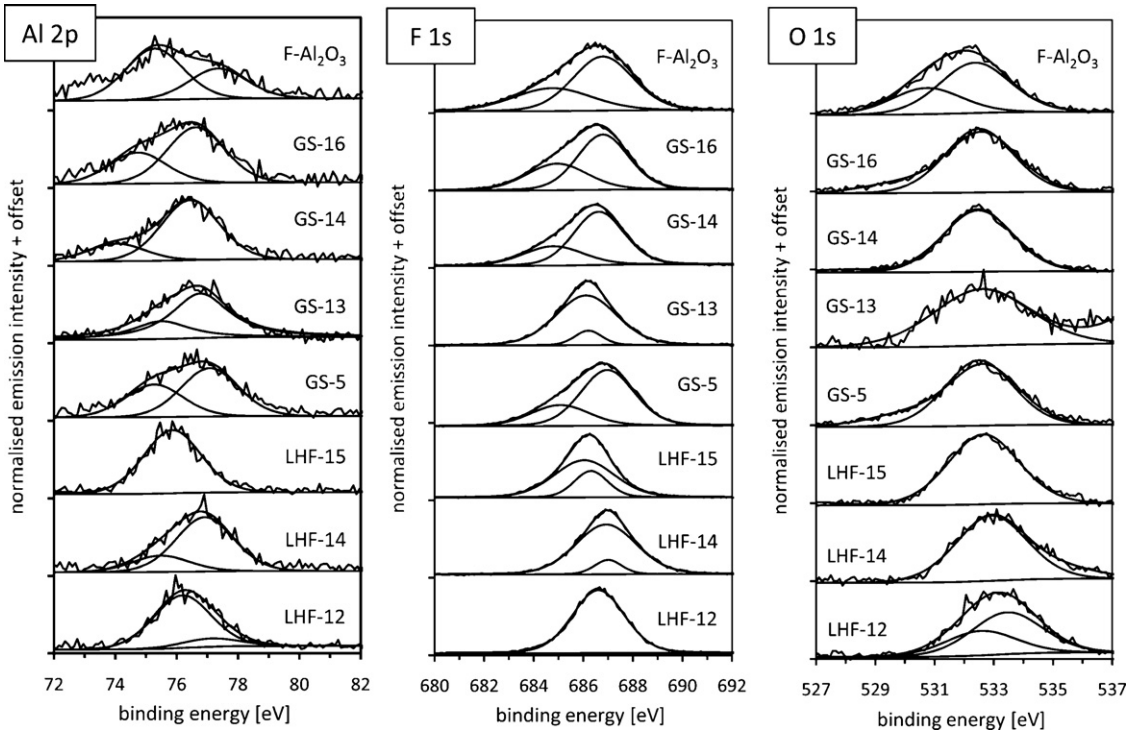

Fig. 1. Al 2p, F 1s and O 1s X-ray photoemission spectra of selected LHF and GS samples in comparison to data for the fluorinated Al_2O_3 sample. Shirley background functions, Gauss–Lorentz curve fits and the resulting spectral envelope are superimposed on the experimental data.

adsorbed water molecules that could only be avoided if samples were consistently handled under ultra-high vacuum conditions. It seems likely that the evacuation treatment causes desorption of H_2O/OH^- and/or HF/F^- species originally present on the surfaces, as previously observed for HS-AlF_3 [8]. Post-treated compounds are thus expected to have higher crystallographic order and hence more regular local coordination of Al^{III} by 6 F neighbours, which would contribute to the observed shift towards higher Al 2p binding energy. As recently shown, removal of hydroxylic surface groups results in a similar Al 2p BE shift towards the value observed for stoichiometric α-AlF_3 [28]. Computational studies of AlF_3 surfaces suggest that a shift to higher BE could also be due to the formation of under-coordinated Lewis acid sites. However, the distortions in AlF_3 octahedra observed in HS-AlF_3, synthesised *via* the sol–gel route, caused a lowering of the Al 2p BE compared to crystalline octahedral AlF_3 forms [7,8].

The O 1s spectra of all LHF are dominated by a broad emission feature centred at a binding energy of approximately 533 eV, which is attributable to hydroxyl groups (Table 2, Fig. 1) [28]. The O 1s emission of the high surface area samples that had been evacuated after synthesis, LHF-12 and LHF-14, is somewhat broader, with a high-binding energy tail extending to 536 eV, which is likely due to adsorbed water [28–31]. The possible origins of OH groups and water, which were also identified by FTIR spectroscopy, will be discussed below.

As indicated in Section 2, the precursor, $[N_2H_6][AlF_5]$, could contain up to 2 wt.% of residual water, even after drying at 393 K. It is known that in the $HF–H_2O–AlF_3$ superacid medium oxonium fluoroaluminates(III) are formed [32]. From our experience and observations made by others [33], oxonium ions are quite resistant to strong oxidisers. It is therefore very likely that under the oxidative conditions used in the preparations water or other oxygen-containing species present in the precursor will not be converted to HF and oxygen but will remain in the reaction mixture in the form of chemically stable oxonium species. On post-treatment at 523 K, routinely performed on all batches, the

Table 2
XPS binding energies and FWHM values for AlF_3 samples prepared by F_2 treatment in aHF solution (LHF-samples). All fits were obtained by entirely unconstrained fitting of two Gauss–Lorentz peaks as described in the text.

Sample	Binding energies/eV (FWHM/eV)					
	Al 2p		O 1s		F 1s	
	Low BE	High BE	Low BE	High BE	Low BE	High BE
LHF-15 (raw product)	75.9 (2.2)	–	532.6 (2.7)	–	686.0 (2.9)	686.3 (1.6)
LHF-14	76.7 (2.2)	–	532.9 (2.7)	–	686.9 (2.9)	687.0 (1.3)
LHF-12	76.3 (2.2)	–	532.6 (2.7)	533.5 (2.7)	686.6 (2.5)	–

Table 3
Binding energy and FWHM values for low surface area AlF_3 samples (GS-samples) and for fluorinated γ-alumina. All fits were obtained by entirely unconstrained fitting of two Gauss–Lorentz peaks as described in the text.

	Binding energies/eV (FWHM/eV)					
	Al 2p		O 1s		F 1s	
	Low BE	High BE	Low BE	High BE	Low BE	High BE
F–Al_2O_3	75.3 (2.2)	77.3 (2.2)	530.7 (2.7)	532.4 (2.7)	684.8 (3.8)	686.8 (2.9)
GS-5	75.3 (2.2)	77.1 (2.2)	–	532.5 (2.7)	685.1 (2.8)	687.0 (2.5)
GS-13	74.9 (2.2)	76.7 (2.2)		532.6 (2.7)	686.1 (2.9)	686.2 (1.3)
GS-14	74.0 (2.2)	76.4 (2.2)	–	532.5 (2.7)	684.8 (2.9)	686.6 (2.4)
GS-16	74.7 (2.2)	76.6 (2.2)	–	532.5 (2.7)	685.0 (2.9)	686.8 (2.4)

oxonium salts will thermally decompose with release of HF and H_2O. This is a possible route to hydration and hydroxylation of the AlF_3 surface. Another possibility is the adsorption of water during the transfers required to obtain XPS and FTIR spectra. A clear differentiation between the oxygen species originating from these two sources is therefore not possible and for this reason, no attempt was made to estimate the quantities of hydroxyl groups present in the various samples examined.

The F 1s binding energies of the non-evacuated AlF_3 compound, LHF-15, Table 2, is significantly lower, at about 686.0–686.3 eV, than for LHF-12 and LHF-14 (686.6–687.0 eV). For LHF-14 and LHF-15 there is also an indication of heterogeneity, likely between stoichiometric ordered domains and non-stoichiometric hydroxylated domains, through a bimodal peak shape consisting of two peak component at almost equal binding energies. A less intense low FWHM component is superimposed over a dominant component with high FWHM. The binding energies of all these F 1s peaks are indicative for the presence of fluoride ions, as found for other aluminium fluorides [16,34,35]. However, slightly higher F 1s binding energies of the post-synthesis treated samples (LHF-12 and LHF-14) are likely to have their origin in a more stoichiometric fluoride, caused by removal of OH groups and water. This conclusion is supported by the fact that the intensity of the O 1s emission of LHF-14 and LHF-12 was significantly weaker than for LHF-15. Ordering of the crystal structure by the applied heat treatment may contribute as well, as indicated by the increasingly strong low-FWHM component in the F 1s data of the post-synthesis treated samples, which indicates that heterogeneity develops through the beginning growth of a more ordered and stoichiometric phase. Finally, thermal removal of HF may also contribute to improvements in stoichiometry and order.

3.2.2. Low surface area samples (GS samples)

For the GS samples and the F-alumina reference, the Al 2p photoemission peak had to be fitted with two GL curves (Table 3). The FWHM for each component was constrained to 2.2 eV. The binding energy of the Al 2p low energy component is between 74.0 and 75.3 eV and is likely to be associated with the oxide- and hydroxyl-coordinated species, with the variation in binding energy among the examined samples likely due to varying degrees of incomplete fluorination, but distortions of the crystal structure and/or coordination numbers may also contribute. The binding energy of the high energy component of the Al 2p emission spectra varies between 77.3 and 76.4 eV. It is in the range expected for the Al 2p binding energy of Al fluorides, for example for six-fold coordinated α-AlF_3 [36]. A complicating feature of the analysis is that despite similarity in the synthesis routes used, differences in the resultant structure may occur because of difficulty in controlling heat dissipation under gas–solid reaction conditions.

The fluorinated γ-alumina reference material, F–Al_2O_3, Tables 1 and 3, also has two Al 2p components. This observation differs from results obtained in a previous study of γ-alumina fluorinated using $CHClF_2$ or CHF_3 [31]. However, it should be noted that the previous data were obtained with a different instrument and exhibited significantly higher FWHMs for individual peaks; it is therefore possible that the two components were previously not resolved. Fluorination of the surface is a slow process, the initial uptake of F occurring at the surface of oxide particles and subsequently F being inserted into sub-surface regions of the crystallites [31]. As for the GS samples discussed above, the low binding energy of the Al 2p peak can be assigned to aluminium bound primarily to oxygen, an environment relating closely to γ-alumina, and the high BE component to an aluminium in a partially fluorinated environment [28]. It is not necessary to postulate the existence of a homogeneous ordered, oxofluoride phase, for example related to that recently identified as an intermediate during the pyrohydrolysis of α-AlF_3 [37].

The O 1s photoemission peak for the samples from the GS group has been fitted with one GL curve and for the F–Al_2O_3 reference material with two GL curves, with the FWHM constrained to 2.7 for all components (Table 3). All low surface area AlF_3 samples contain an O 1s peak at approximately 532.5 eV which is characteristic for OH^- groups adsorbed on the surface [8,28,30,31,38]. The same features were observed for HS-AlF_3 synthesised *via* the sol–gel route [8] and can be attributed to the hydration of highly Lewis acid surface sites during brief exposures to ambient atmosphere [1,7]. As discussed above for the LHF-samples, there are two possibilities to account for the observed phenomenon here. The low binding energy O 1s component of F–Al_2O_3, visible at 530.7 eV, is almost certainly associated with unreacted γ-Al_2O_3 [31].

The F 1s photoemission peaks have two components. A high binding energy component characteristic of fluoride species [8,16,28,34,35] is dominant and occurs at approximately 686.5 eV (Table 3, Fig. 1). With the exception of GS-13, which appears to have a well ordered and a less ordered fluoride component similar to LHF-14 (see previous section), most of the peaks are asymmetric with a second component on the low BE side. Thus, the presence of another fluorine component cannot be excluded especially for the reference material, F–Al_2O_3, which shows the most pronounced F 1s shoulder that may be the result of two different F/O environments. When O is present, redistribution of electron density may occur from O *via* Al^{III} centres to F. As a result, the electron density at F would be increased, lowering the F 1s binding energy. Since the O 1s spectra for F–Al_2O_3 indicated the presence of oxidic species at the surface it seems likely that their influence on the F 1s emission is present.

3.3. Catalytic activity

3.3.1. Catalytic activity w.r.t. isomerisation of 1,1,2-trichlorotrifluoroethane and the subsequent dismutation reactions

The isomerisation of CCl_2FCClF_2 to give the thermodynamically more stable isomer, CCl_3CF_3 has a long history. The reaction forms part of the large scale process for chlorofluorocarbon synthesis, whereby chloroethanes were fluorinated by aHF vapour in the presence of fluorinated chromia as an heterogeneous catalyst. In contrast to the other steps of the process, the isomerisation of CCl_2FCClF_2 proceeds by an intramolecular pathway in which catalyst surface F and Cl species are not involved [39]. The isomerisation, carried out under reflux in the presence of solid aluminium trichloride, was also the first stage in an industrial process used for many years to prepare the synthetic intermediate, CCl_3CF_3. In reality, the heterogeneous catalyst is not solid $AlCl_3$ but solid aluminium chlorofluoride, ACF [14,15], which is formed *in situ* [40,41]. It is ACF therefore that is the archetypal heterogeneous catalyst for this reaction against which other aluminium fluoride catalysts should be compared. Dismutation of CCl_3CF_3 to give a 1:1 mixture of CCl_2FCF_3 and CCl_3CClF_2 occurs over Lewis acidic aluminium-containing catalysts [13,24]; [^{36}Cl] radiotracer studies are consistent with Cl and F transfers between two CCl_3CF_3 adsorbed at β-aluminium trifluoride without the intervention of surface halogen atoms [24,42]. This dismutation reaction implies the existence of an interaction, $Al^{\delta+}$–F–C [13].

Product distributions at various temperatures resulting from the catalytic behaviour of the high surface AlF_3-based LHF-materials, two reference materials, F–Al_2O_3 and β-AlF_3, used in previous studies of this reaction [13,24], and two highly acidic reference catalysts, aluminium chlorofluoride (ACF) [14,15] and sol–gel derived high surface area AlF_3 (HS-AlF_3) [1] are shown in Fig. 2. A logarithmic ordinate axis scale is used for better visualisation of minor products. The products observed are most

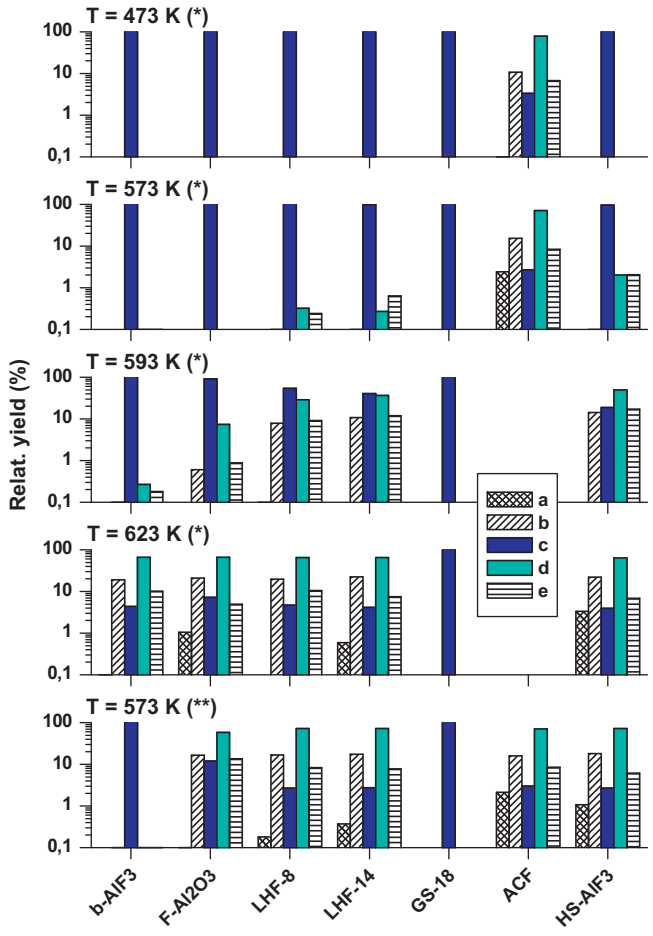

Fig. 2. CCl_2FCClF_2 isomerisation tests: product composition at different temperatures for three newly synthesised materials (LHF-8, LHF-14, GS-18) in comparison with conventional reference catalysts, β-AlF_3 and fluorinated γ-alumina (F–Al_2O_3), and highly acidic materials, aluminium chlorofluoride (ACF) and sol–gel derived high surface area AlF_3 (HS-AlF_3). Residence time is 1s; feed is 10 vol.% CCl_2FCClF_2 in N_2; (*) activation steps, (**) after activation. Legend: a – $CClF_2CF_3$, b – CCl_2FCF_3, c – CCl_2FCClF_2, d – CCl_3CF_3, e – CCl_3CClF_2.

obviously rationalised on the basis of Eqs. (4)–(6), in which the letters in parentheses relate to the blocks in Fig. 2.

$$\underset{(c)}{CCl_2FCClF_2} \rightarrow \underset{(d)}{CCl_3CF_3} \quad (4)$$

$$2\underset{(d)}{CCl_3CF_3} \rightarrow \underset{(b)}{CCl_2FCF_3} + \underset{(e)}{CCl_3CClF_2} \quad (5)$$

$$2\underset{(b)}{CCl_2FCF_3} \rightarrow \underset{(a)}{CClF_2CF_3} + \underset{(d)}{CCl_3CF_3} \quad (6)$$

In addition to CCl_3CF_3, (d) in Fig. 2, and unchanged CCl_2FCClF_2 (c), the expected dismutation products from Eq. (5), CCl_2FCF_3 (b) and CCl_3CClF_2 (e), are observed. In most cases $CClF_2CF_3$ (a) is a minor product, suggesting that the dismutation of CCl_2FCF_3, Eq. (6), is less facile that that of CCl_3CF_3, Eq. (5). At the highest activation temperature examined, 623 K, and at 573 K after activation the observed yields of CCl_3CClF_2 (e) are less than expected but the reasons for this anomaly were not explored.

Only ACF is active at 473 K, the lowest initial temperature that was studied. Pronounced carbonisation of the ACF catalyst was apparent after the reaction, indicating decompositions that could be the result of the highly acidic surface [15]. The activities of all other materials examined are lower; they all need activation at ≥573 K. Of the AlF_3 samples newly prepared in the present work, samples LHF-8 and LHF-14 have activities at 593 K rather comparable to that of sol–gel prepared, HS-AlF_3 and superior to reference materials, F–Al_2O_3 and β-AlF_3. However, differences in catalytic behaviour of all active materials level out at 623 K. After activation at 623 K, catalysts, with the exemption of β-AlF_3, are active at 573 K. For the two reference materials, F–Al_2O_3 and β-AlF_3, the observed behaviour is in complete agreement with a previous study [24] where the onset of catalytic activity above 590 K for β-AlF_3 and above 520 K for fluorinated alumina materials was determined. Very similar isomerisation activity is observed at 573 K for the four most active catalysts, LHF-8, LHF-14, HS-AlF_3 and ACF. Differences between them become more pronounced when the reaction temperature is further lowered (not shown in Fig. 2); LHF-8 is inactive at temperatures below 523 K while HS-AlF_3 and ACF retain some activity at 423 K, the lowest final temperature employed in our study. In general, the present study confirms the high isomerisation activity of the latter two catalysts, although at slightly higher temperatures than the 323–373 K range reported earlier [41]. Discrepancies between the two studies may be, at least in part, attributed to the minor differences in experimental conditions, i.e. contact time and temperature regime, but more importantly to the fact that the authors of [41] used freshly prepared active catalysts that exhibited immediate activity. In contrast, HS-AlF_3 used in the present study needed a distinctive activation step to achieve full activity. Activation processes are discussed at the end of the section.

Somewhat unexpectedly, the samples prepared under gas–solid conditions, illustrated by GS-18 in Fig. 2, were completely inactive in CCl_2FCClF_2 isomerisation over the whole temperature range tested. This is not simply the result of low specific surface areas, in view of the catalytic activity observed for F–Al_2O_3 above 593 K (Fig. 2); the BET area of F–Al_2O_3 is relatively small (Table 1). It is suggested that the catalytic inactivity of GS-AlF_3 samples can be explained by a combination of the formation of partially crystallised AlF_3 phases, similar to α-AlF_3, that have low surface areas, and the presence of residual $[NH_4]^+$ bulk species, for example sample GS-5 (Table 1). The presence of $[NH_4]^+$ also acts as a catalyst poison in some LHF samples; for example the as-prepared LHF-15 and LHF-16 (Table 1, Fig. 3) were inactive w.r.t. isomerisation of CCl_2FCClF_2. Furthermore, adding a small amount of $[NH_4][AlF_4]$ to an active AlF_3 material (sample LHF-14, Fig. 2 and Table 1) inhibited completely its activity.

Strategies to reduce residual $[NH_4]^+$ to acceptable levels were therefore investigated. The procedure by which the liquid aHF phase is removed from the reaction vessel after $[N_2H_6][AlF_5]$ decomposition is one important factor; lower amounts of $[NH_4]^+$ were indicated when the liquid aHF phase was decanted rather than pumped off. The $[NH_4]^+$ containing impurities are soluble in liquid aHF at least to some extent and can be removed by decantation. For example, multiple extractions from a catalytically inactive sample (LHF-15, Fig. 3) with liquid aHF resulted in a catalytically active material with a lower $[NH_4]^+$ content being indicated qualitatively from its IR spectrum (sample LHF-15a, Fig. 3). Additional decrease in $[NH_4]^+$ was observed also after CCl_2FCClF_2 isomerisations at 623 K (sample LHF-15a-1, Fig. 3).

Although reduction of the $[NH_4]^+$ content was indicated after post treatment of LHF-15 with F_2 under UV-irradiation in aHF at room temperature (sample LHF-15b, Fig. 3), this was evidently insufficient to result in catalytic activity. Conversion of inactive to catalytically active material was also achieved in some cases by treatment of a sample with CCl_2F_2 at 623 K. Treatment of sample LHF-16, which displayed no activity w.r.t. CCl_2FCClF_2 isomerisation by CCl_2F_2 flow at 623 K resulted in an active catalyst, despite the reduction in BET area, 217–125 $m^2\,g^{-1}$ (sample LHF-16a, Table 1, Fig. 3).

With the exception of ACF, an activation period was required before maximum catalytic activity was achieved. Only the

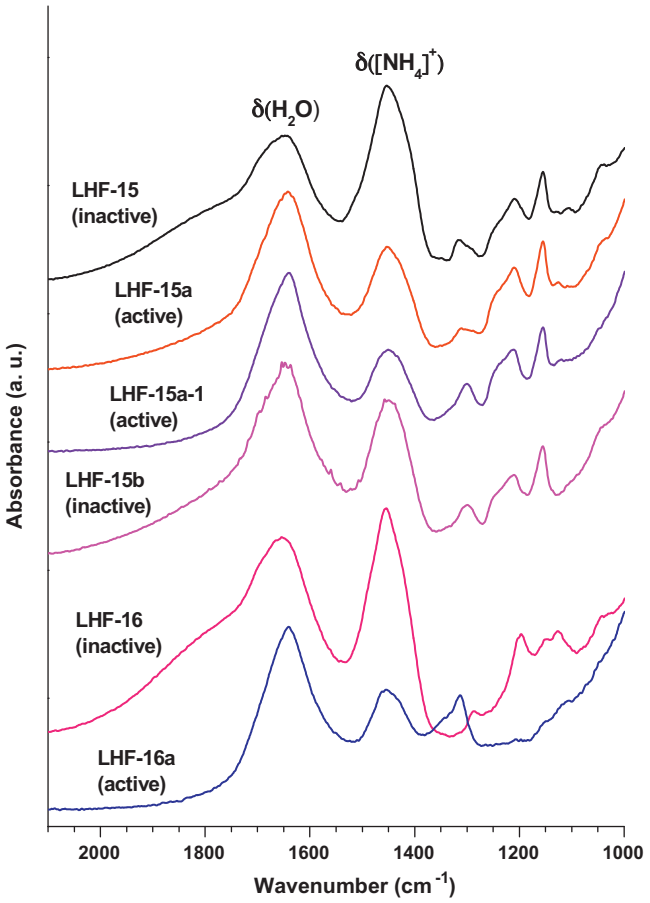

Fig. 3. Normalised PA IR spectra of materials from oxidative decomposition of $N_2H_6AlF_5$ in liquid aHF showing qualitatively, the effect of the post-treatments on the $[NH_4]^+$ levels and catalytic activity in CCl_2FCClF_2 isomerisation. LHF-15 and LHF-16: as-prepared materials; LHF-15a: after additional extractions with liquid aHF; LHF-15a-1: LHF-15a after CCl_2FCClF_2 isomerisation test; LHF-15b: treated with F_2 in liquid aHF under UV-irradiation; LHF-16a: treated with CCl_2F_2 at 623 K.

activated LHF-materials, F–Al_2O_3 and HS-AlF_3 show high catalytic activity at 573 K with no loss of performance during several hours on-stream. Treatment, using an HFC or HCFC is known to result in partial fluorination of an alumina surface [11,43,44], and fluorination of aluminium alkoxide-derived fluoride gels with an HCFC or CFC is a route to HS-AlF_3 [1]. In view of the combined XPS and FTIR results described above, it is tempting to suggest that treatment with the CFCs, CCl_2F_2 or CCl_2FCClF_2, is a way of decreasing the concentration of both, surface hydroxyl groups and $[NH_4]^+$ species, leading to catalytic activity, with an increase in the concentration of accessible Lewis acid sites on the surface.

3.3.2. Catalytic activity w.r.t. dehydrochlorination of tert-butyl chloride

Following the discovery that the interactions involving the solid Lewis acid, β-AlF_3 with anhydrous HCl and Bu^{t}Cl vapours could be observed at room temperature [45], by means of an *in situ* Geiger Müller direct surface monitoring technique and [^{36}Cl]-labelled probes, the method has been used to test for the presence of surface Lewis acid sites in ACF [25], HS-AlF_3 and HS-MgF_2 sol–gel synthesised materials [9] and the HTB-structured, aluminium hydroxy fluoride, $AlF_{2.6}(OH)_{0.4}$ [26]. In essence, H^{36}Cl produced by surface-catalysed dehydrochlorination of [^{36}Cl]-Bu^{t}Cl becomes adsorbed at the surface, very often chemically adsorbed although the geometry of the adsorbed state must be inferred rather than be determined from the radiotracer method. The strong point of the method is its sensitivity; when the extent of Bu^{t}Cl dehydrochlorination is significant, HCl can be detected in the gas phase above the surface by FTIR [25]. This is possible for HS-AlF_3 but not for the less effective solid Lewis acids, HS-MgF_2 or $AlF_{2.6}(OH)_{0.4}$ [9,26].

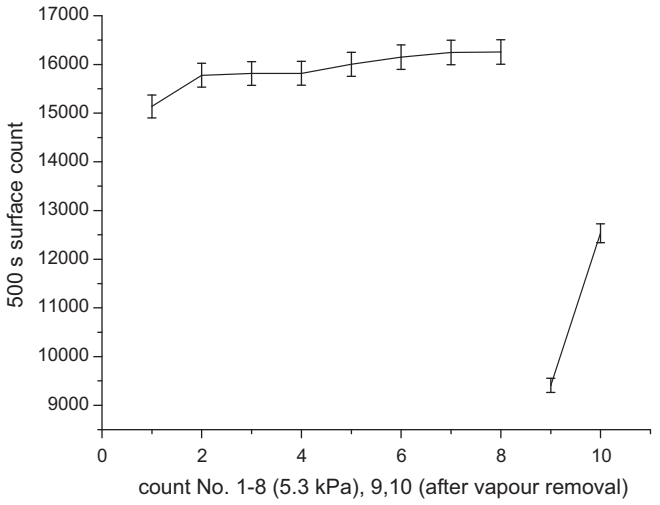

Fig. 4. Surface counts from HS-AlF_3 (LHF-12), synthesised *via* the liquid aHF route, during exposures to aliquots of [^{36}Cl]-labelled Bu^{t}Cl. The line break corresponds to the removal of the final aliquot of vapour; count 9 was recorded immediately after vapour removal and count 10 5 d later.

Exposure of the AlF_3 sample, LHF-12 (Table 1) successively to a series of aliquots of [^{36}Cl]–Bu^{t}Cl vapour led to the [^{36}Cl] surface count data in Fig. 4.

For this sample (BET area = 276 m^2 g^{-1}) the mean surface count over eight additions of [^{36}Cl]–Bu^{t}Cl was 15,900 ± 364 (2.3%). Although the surface [^{36}Cl] activity appears to show a small increase with successive additions, this may not be significant. Removal of vapour and weakly adsorbed species after count No. 8 resulted in a large decrease in surface count, albeit not to the background value. After 5 d in vacuo with intermittent pumping there is a significant increase in the surface count (count No. 10). This type of behaviour has been observed with other Al^{III} and with Mg^{II} fluoride derivatives that have been exposed either to H^{36}Cl or to [^{36}Cl]–Bu^{t}Cl [9,25,26]; it is a reflection of the small particulate (nanoscopic) nature of the solids and self-absorption of the emitted β^- radiation from [^{36}Cl] [46]; the phenomenon was observed for the other samples examined in the present work. Concomitantly with the increase in surface count, a brick red colouration developed in the sample. A second sample of LHF-12 behaved in an identical fashion to count Nos. 1–9 in Fig. 4.

In order to explore any possible effects on dehydrochlorination ability of a pre-treatment with CCl_2F_2, the behaviour of two AlF_3 samples from the same batch, LHF-16 and LHF-16(a), Table 1, towards exposure to [^{36}Cl]–Bu^{t}Cl was examined. The samples LHF-16(a), as received, were dark red-green in colour; their BET area was 125 m^2 g^{-1}, significantly smaller than that of the samples, LHF-16, which were 217 m^2 g^{-1} (Table 1) and which were off-white in colour.

Comparison between the two experiments indicates that treatment of sample LHF-16 with CCl_2F_2 to give LHF-16a, does not inhibit obviously its activity with respect to dehydrochlorination of [^{36}Cl]–Bu^{t}Cl. The decrease in specific surface area resulting from the pre-treatment does, however, lead to less precise determinations of the [^{36}Cl] surface counts. In the absence of a pre-treatment, the behaviour observed for LHF-16 is very similar to that described for sample LHF-12 in Fig. 4. In both cases retention of H^{36}Cl is substantial, in agreement with the results of direct exposures of H^{36}Cl to LHF-16(a) and LHF-16, shown in Fig. 5(a) and (b).

There is some evidence, apparent also from the [^{36}Cl] surface count relationships that result from exposure of the two samples to

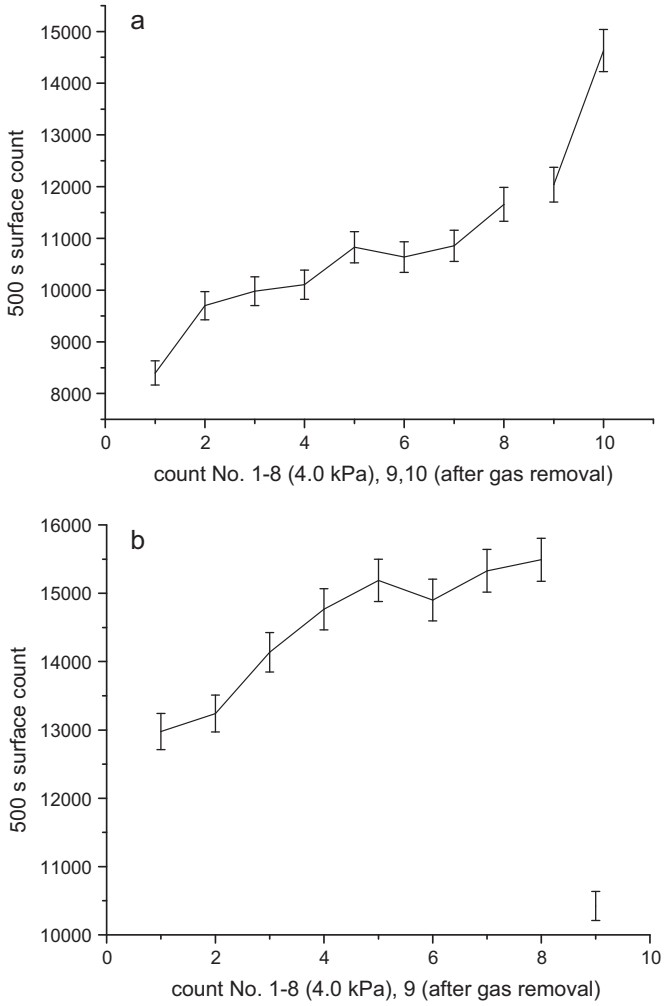

Fig. 5. Surface counts from HS-AlF_3 (LHF-16a and -16), synthesised *via* the liquid aHF route, during exposures to aliquots of anhydrous $H^{36}Cl$. The line breaks correspond to the removal of the final aliquot of gas. (a) The sample had been treated with CCl_2F_2 to promote CCl_2FCClF_2 isomerisation activity; (b) the sample received no CCl_2F_2 treatment; in (a) count 10 recorded 24 h after count 9.

$H^{36}Cl$ aliquots directly, Fig. 5(a) and (b) that the CCl_2F_2 pre-treatment results in the retention of a greater proportion of $H^{36}Cl$ both at the exterior and interior surfaces. Retention of strongly bound HCl, either from dehydrochlorination of Bu^tCl or after direct exposure of an acidic fluoride or oxofluoride surface has been observed on several occasions, for example in [^{36}Cl] experiments that involved sol–gel prepared, HS-AlF_3 and HS-MgF_2 [9]. Depending on the circumstances, dissociative or associative adsorption of HCl is possible and the various possibilities on oxides, fluorides and oxofluorides have been described [47]. In the case being considered here (sample LHF-16 and -16a), HCl could be dissociatively adsorbed, at surface hydroxyl groups, for H^+, and at strongly Lewis acid Al^{III} centres, for Cl^-, or associatively adsorbed at Al^{III} centres. If it is assumed that CCl_2F_2 treatment reduces the surface concentration of –OH groups, as proposed above, when considering the behaviour observed for strongly retained $H^{36}Cl$, for example in Fig. 5(a) and (b), it can be concluded tentatively that an important component is associatively adsorbed $H^{36}Cl$ at strongly Lewis acid Al^{III} sites.

Although there was no evidence that the samples prepared *via* the gas–solid conditions route had any catalytic activity in room temperature Bu^tCl dehydrochlorination, interaction with $H^{36}Cl$ could be detected, albeit with low precision. For example, the behaviour of sample, GS-33, specific surface area = 22 $m^2\ g^{-1}$, indicates that the interaction does not consist solely of physical adsorption of $H^{36}Cl$; a substantial fraction is strongly adsorbed at the surface.

4. Conclusions: comparisons among HS-AlF_3 samples prepared by oxidative decomposition and sol–gel routes

The AlF_3 samples prepared in this work illustrate very well the effect of specific surface area on the concentration of surface sites that show Lewis acidity. A correlation has been established for other Al^{III} fluoride derivatives [48]; it appears that the AlF_3 samples studied here fit this concept, at least qualitatively.

The decomposition of $[N_2H_6][AlF_5]$ in the presence of F_2 and aHF is a viable alternative route to the preparation of HS-AlF_3, providing the post treatment regime is successful in removing $[NH_4]^+$ salts which are formed as a result of an incomplete redox reaction. If this is not achieved, Lewis acid sites appear to be blocked with a consequent effect on catalytic activity.

XPS provides convincing evidence for the presence of surface hydration and hydroxylation. The effects on the XPS data are very similar to those observed in HS-AlF_3 prepared *via* the sol–gel-then-fluorination route [8]. In the present case hydration/hydroxylation may be the result of brief exposure to ambient atmosphere [8] but in addition small quantities of water originating from the AlF_3 precursor, could be the source. No attempt has been made to quantify the surface hydroxyl groups; it is concluded however that their effect can be reduced, for example, the effect of CCl_2F_2 surface treatment is rationalised as a way of replacing surface Al–OH by Al–F. It results also in an increase in the number of Lewis acid surface sites.

Acknowledgements

We thank Prof. Dr. E. Kemnitz (HU-Universität, Berlin) for the provision of samples and the EU for support of this work through the 6th Framework Programme (FUNFLUOS, contract No. NMP3-CT-2004-5005575). AM held a Marie-Curie Fellowship awarded through the EXPERT programme funded by the EU at The University of Manchester under the 6th Framework Programme. Part of the work done in Ljubljana was also funded by the Slovenian Research Agency (research programme Inorganic Chemistry and Technology; P1-0045).

References

[1] E. Kemnitz, U. Groβ, St. Rüdiger, S. Chandra Shekar, Angew. Chem. Int. Ed. 42 (2003) 4251–4254;
K. St. Ruediger, U. Groβ, M. Feist, H.A. Prescott, S. Chandra Shekar, S.I. Troyanov, E. Kemnitz, J. Mater. Chem. 15 (2005) 588–597;
St. Rüdiger, G. Eltanany, U. Groβ, E. Kemnitz, J. Sol–Gel Sci. Technol. 41 (2007) 299–311;
St. Rüdiger, U. Groβ, E. Kemnitz, J. Fluorine Chem. 128 (2007) 353–368;
T. Krahl, A. Vimont, G. Eltanany, M. Daturi, E. Kemnitz, J. Phys. Chem. C 111 (2007) 18317–18325.
[2] J. Krishna Murthy, U. Groβ, St. Rüdiger, E. Kemnitz, J.M. Winfield, J. Solid State Chem. 179 (2006) 739–746;
St. Wuttke, G. Scholz, St. Rüdiger, E. Kemnitz, J. Mater. Chem. 17 (2007) 4980–4988.
[3] St. Rüdiger, E. Kemnitz, Dalton Trans. (2008) 1117–1127;
E. Kemnitz, St. Rüdiger, in: A. Tressaud (Ed.), Functionalized Inorganic Fluorides: Synthesis, Characterization & Properties of Nanostructured Solids, John Wiley & Sons Ltd, Chichester, 2010, pp. 69–99.
[4] A. Rahten, P. Benkič, A. Jesih, Acta Chim. Slov. 46 (1999) 339–354.
[5] S. Milićev, A. Rahten, Eur. J. Solid State Inorg. Chem. 28 (1991) 557–566.
[6] T. Skapin, G. Tavčar, A. Benčan, Z. Mazej, J. Fluorine Chem. 130 (2009) 1086–1092.
[7] N. Weiher, A. Makarowicz, A.M. Beesley, E. Kemnitz, S.L.M. Schroeder, X-ray Absorption Fine Structure 13th International Conference, AIP Conference Proceedings, vol. 882, (2007), pp. 827–829.
[8] A. Makarowicz, C.L. Bailey, N. Weiher, E. Kemnitz, S.L.M. Schroeder, S. Mukhopadhyay, A. Wander, B.G. Searle, N.M. Harrison, Phys. Chem. Chem. Phys. 11 (2009) 5664–5673.

[9] M. Nickkho-Amiry, G. Eltanany, St. Wuttke, St. Rüdiger, E. Kemnitz, J.M. Winfield, J. Fluorine Chem. 129 (2008) 366–375.
[10] R. Weinland, I. Lang, A. Fikentscher, Z. Anorg. Allg. Chem. 150 (1926) 47–67.
[11] T. Skapin, J. Mater. Chem. 5 (1995) 1215–1222.
[12] T. Skapin, E. Kemnitz, Catal. Lett. 40 (1996) 241–247.
[13] H. Bozorgzadeh, E. Kemnitz, M. Nickkho-Amiry, T. Skapin, J.M. Winfield, J. Fluorine Chem. 110 (2001) 181–189.
[14] T. Krahl, R. Stösser, E. Kemnitz, G. Scholz, M. Feist, G. Silly, J.-Y. Buzaré, Inorg. Chem. 42 (2003) 6474–6483.
[15] T. Krahl, E. Kemnitz, J. Fluorine Chem. 127 (2006) 663–678.
[16] A. Le Bail, C. Jacoboni, M. Leblanc, R. De Pape, H. Duroy, J.L. Fourquet, J. Solid State Chem. 77 (1988) 96–101.
[17] R. Pribil, Applied Complexometry, Pergamon Press, Oxford, 1982, pp. 171–178.
[18] M. Ponikvar, B. Sedej, B. Pihlar, B. Žemva, Anal. Chim. Acta 418 (2000) 113–118.
[19] M. Ponikvar, B. Žemva, J.F. Liebman, J. Fluorine Chem. 123 (2003) 217–220.
[20] A.I. Vogel, Textbook of Quantitative Inorganic Analysis: Including Elementary Instrumental Analysis, 4th ed., Longman, London, 1978, pp. 313–314, 687–690.
[21] HACH DR/2010 Spectrophotometer Handbook.
[22] N. Fairley, A. Currick, The CASA Cookbook: Recipes for XPS Data Processing Pt. 1, 2003.
[23] C.J. Powell, Appl. Surf. Sci. 89 (1995) 141–149.
[24] H. Bozorgzadeh, E. Kemnitz, M. Nickkho-Amiry, T. Skapin, J.M. Winfield, J. Fluorine Chem. 107 (2001) 45–52.
[25] M. Nickkho-Amiry, J.M. Winfield, J. Fluorine Chem. 128 (2007) 344–352.
[26] D. Dambournet, H. Leclerc, A. Vimont, J.-C. Lavalley, M. Nickkho-Amiry, M. Daturi, J.M. Winfield, Phys. Chem. Chem. Phys. 11 (2009) 1369–1379.
[27] D.-H. Menz, U. Bentrup, Z. Anorg. Allg. Chem. 576 (1989) 186–196.
[28] Chr. Stosiek, G. Scholz, S.L.M. Schroeder, E. Kemnitz, Chem. Mater. 22 (2010) 2347–2356.
[29] J.A. van Bokhoven, A.M.J. van der Eerden, D.C. Koningsberger, J. Am. Chem. Soc. 125 (2003) 7435–7442.
[30] C.D. Wagner, D.E. Passoja, H.F. Hillery, T.G. Kinisky, H.A. Six, W.T. Jansen, J.A. Taylor, J. Vac. Sci. Technol. 21 (1982) 933–944.
[31] O. Boese, W.E.S. Unger, E. Kemnitz, S.L.M. Schroeder, Phys. Chem. Chem. Phys. 4 (2002) 2824–2832.
[32] D. Mootz, E.-J. Oellers, M. Wiebcke, Acta Cryst. C44 (1988) 1334–1337; I.V. Tananaev, S.P. Gabuda, T.D. Fedotova, A.A. Opalovski, Dokl. Akad. Nauk. SSSR 179 (1968) 362–365.
[33] M. Gerken, M.D. Moran, H.P.A. Mercier, B.E. Pointner, G.J. Schrobilgen, B. Hoge, K.O. Christe, J.A. Boatz, J. Am. Chem. Soc. 131 (2009) 13474–13489.
[34] R. Hoppe, D. Kissel, J. Fluorine Chem. 24 (1984) 327–340.
[35] N. Herron, D.L. Thorn, R.L. Harlow, G.A. Jones, J.B. Parise, J.A. Fernandez-Baca, T. Vogt, Chem. Mater. 7 (1995) 75–83.
[36] G.E. McGuire, G.K. Schweitzer, T.A. Carlson, Inorg. Chem. 12 (1973) 2450–2453.
[37] M. Gaudon, J. Majimel, J.-M. Heintz, M. Feist, D. Dambournet, A. Tressaud, J. Fluorine Chem. 129 (2008) 1173–1179.
[38] A. Hess, E. Kemnitz, A. Lippitz, W.E.S. Unger, D.-H. Menz, J. Catal. 148 (1994) 270–280.
[39] L. Rowley, J. Thomson, G. Webb, J.M. Winfield, A. McCulloch, Appl. Catal. A 79 (1991) 89–103.
[40] D.G. McBeth, M.M. McGeough, G. Webb, J.M. Winfield, A. McCulloch, N. Winterton, Green Chem. 2 (2000) 15–20.
[41] J. Krishna Murthy, U. Groβ, St. Rüdiger, V. Venkat Rao, V. Vijaya Kumar, A. Wander, C.L. Bailey, N.M. Harrison, E. Kemnitz, J. Phys. Chem. B 110 (2006) 8314–8319.
[42] H. Bozorgzadeh, E. Kemnitz, M. Nickkho-Amiry, T. Skapin, G.D. Tate, J.M. Winfield, J. Fluorine Chem. 112 (2001) 225–232.
[43] A. Hess, E. Kemnitz, J. Catal. 149 (1994) 449–457.
[44] J.M. Winfield, J. Fluorine Chem. 130 (2009) 1069–1079.
[45] C.H. Barclay, H. Bozorgzadeh, E. Kemnitz, M. Nickkho-Amiry, D.E.M. Ross, T. Skapin, J. Thomson, G. Webb, J.M. Winfield, J. Chem. Soc.: Dalton Trans. (2002) 40–47.
[46] W.D. Ehmann, D.E. Vance, Radiochemistry and Nuclear Methods of Analysis, John Wiley and Sons, Inc, New York, 1991.
[47] A. Vimont, M. Daturi, J.M. Winfield, in: A. Tressaud (Ed.), Functionalized Inorganic Fluorides: Synthesis, Characterization & Properties of Nanostructured Solids, John Wiley & Sons, Ltd, Chichester, 2010, pp. 135–136.
[48] D. Dambournet, G. Eltanany, A. Vimont, J.-C. Lavalley, J.-M. Goupil, A. Demourgues, E. Durand, J. Majimel, St. Rüdiger, E. Kemnitz, J.M. Winfield, A. Tressaud, Chem. Eur. J. 14 (2008) 6205–6212.